International Journal of Physical Research, 7 (1) (2019) 26-36

SPC

International Journal of Physical Research

Website: www.sciencepubco.com/index.php/IJPR

Research paper

Structural and microstructural study of SnS thin film semiconductor of 0.2<t≤ 0.4 µm thickness for application in a field effect transistor

Thomas Ojonugwa Daniel [1, 2] *, Uno Essang Uno [2], Kasim Uthman Isah [2], Umaru Ahmadu [2]

[1] *Department of Physics/Geology/Geophysics, Alex Ekwueme-Federal University Ndufu-Alike, P.M.B. 1010, Abakaliki, Ebonyi state, Nigeria*
[2] *Department of Physics, Federal University of Technology, P.M.B. 065, Minna, Nigeria*
**Corresponding author E-mail: danielojonugwathomas@gmail.com*

Abstract

SnS semiconductor thin film of 0.20, 0.25, 0.30, 0.35, 0.40 µm were deposited using aerosol assisted chemical vapour deposition (AACV) on glass substrates and were investigated for use in a field effect transistor. Profilometry, X-ray diffraction, Scanning electron microscope and Energy dispersive X-ray spectroscopy were used to characterise the structural and microstructural properties of the SnS semiconductor. The SnS thin film was found to initially consist of a single crystal at thickness of 0.20 to 0.25µm after which it becomes polycrystalline with an orthorhombic crystal structure consisting of Sn and S elements whose composition varied with increase in thickness. The SnS film of 0.4 µm thickness shows a more uniform grain distribution and growth with a crystal size of 60.57 nm and grain size of 130.31 nm signifying an optimum for the as deposited SnS films as the larger grains reduces the number of grain boundaries and charge trap density hence allowing charge carriers to move freely in the lattice thereby causing a reduction in resistivity, increase in conductivity of the films and enhanced energy band gap which are essentially parameters for a semiconductor material for application in a field effect transistor.

Keywords: *Crystal Structure; Grain Boundaries; Scanning Electron Microscopy; Semiconductor; X-Ray Diffraction.*

1. Introduction

Field effect transistors are unipolar three terminal solid state devices employing only the majority charge carriers in the conduction region. The operation of a field effect transistor at a low operating voltage and high carrier concentration is dependent on the choice of semiconductor channel layer material and the gate dielectric among other parameters. This is due to the dependence of the threshold voltage (V_{th}) (voltage required in switching a transistor) and the minimum gate to source voltage differential needed to create a conducting path between the source electrode and the drain electrode on the semiconductor channel material [1].
However, metal oxides, nitrides, carbon nanotubes and organic semiconductor materials have been the only materials that have been widely applied as semiconductor channel layer of field effect transistor. Therefore, the application of other classes of semiconductor solids has become one of the emerging interests for novel electronic phenomena which is essential for the achievement and development of new device applications and tuning of semiconducting properties of materials [2]. The essential factors that are often considered in the investigation of a semiconductor material for transistor application include the presence of suitable band gap energy, high electrical conductivity, ability to deposit the material using a low cost technique and the abundance of the elements in nature all of which are function of the structural and microstructural properties of the semiconductor material [3].
Metal chalcogenides such as Tin (II) sulphide (SnS) and metal dichalcogenides such as Tin (IV) sulphide (SnS_2) are of interest as potential candidates for the semiconductor channel of field effect transistor. These materials have also been reported for use in solar cells, photoconductive materials, thermoelectric materials and rewritable memory. SnS is abundance in the earth's crust with an orthorhombic structure, it does not contain any toxic or expensive elements; it is a p type semiconducting material with carrier concentration on the order of $10^{16}cm^{-3}$, hole mobility of 1.4 $cm^2V^{-1}s^{-1}$ among other parameter [4-5]. SnS thin film is relatively unexplored for application in a field effect transistor, as literatures pertaining to the application of SnS as semiconductor or transport channel of a field effect transistor is relatively scanty.
Hence in light of these properties of SnS thin film it could be investigated for the feasibility usage of the chalcogenides as semiconductor transport channel of a field effect transistor and to determine the optimum deposition parameters that will give suitable properties for its usage since the SnS thin film has been rarely reported for use as a semiconductor in a field effect transistor. Since the semiconductor thickness can be tuned to achieve desired semiconductor properties, it is chosen as a parameter of interest. The investigation and control of film thickness is important in semiconductor processing as the film thickness influences the surface crystallinity, crystallite size and

Copyright © Thomas Ojonugwa Daniel et al. This is an open access article distributed under the Creative Commons Attribution License, which permits unrestricted use, distribution, and reproduction in any medium, provided the original work is properly cited.

grain size and grain boundary distribution which are essential in defining the electrical and optical band gap of a semiconductor material. The effect of thin film thickness on semiconductor material properties depends also on the method of deposition while the different thin film transistor fabrication methods requires different and specific optimum semiconductor thickness for its ideal operation and easy reproducibility [6]. The deposition method of interest in the study is the aerosol assisted chemical vapour deposition (AACVD). AACVD offers the competitive advantage of usage of less-volatile precursors, thus widening the types of molecules that can be used to deposit thin films.
A thickness range of 0.20-0.40 μm was selected from the average values and method of thickness variation obtained in literatures for the semiconductors applied in the fabrication of a field effect transistor. Preliminary deposition and profilometry was carried out to determine the starting precursor concentrations to achieve the thickness range and also the substrate temperature to use. Hence the study focuses on the structural and microstructural study of SnS thin film semiconductor material of $0.2< t \leq 0.4$ μm thickness for application in a field effect transistor

2. Experimental procedure

Soda lime glass substrates were cleaned using the cleaning methods described as follows: a. the substrates were washed in sodium lauryl sulphate (SLS) solution to remove oil and protein. b. to remove the organic contaminants, the substrates were immersed in piranha solution (H_2SO_4: H_2O_2 (3:1)) for 30 minutes. c. the substrates were then ultrasonically cleaned in distilled water using a sonicator and kept in methanol until it is ready to be used. d. Finally, to use the substrate for deposition process, the substrate were taken from the methanol and dried in air at 150℃. The SnS semiconductor thin films of varying thickness were each deposited using 0.1 M Tin chloride dehydrates and 0.2 M of Thiourea which were weighed in stoichiometric proportion and dissolve in ethanol solvent. The two solutions were then mixed and stirred for 1 hour using a magnetic stirrer at room temperature and then deposited on the substrate by aerosol assisted chemical vapour deposition (AACVD) at a constant substrate temperature of 258 ℃, nozzle distance of 6.8 mm, substrate to nozzle distance of 3 cm, spray volume of 0.2 mL and spray rate of 0.04 ml/min. Five samples of SnS thin films were deposited at thickness of 0.4 μm, 0.35 μm, 0.30 μm, 0.25 μm and 0.20 μm (Labelled as Sample 2, Sample 3, Sample 4, Sample 5 and Sample 6) which was achieved by keeping the initial concentration of the SnS precursors constant using 1 ml of the precursor while varying the concentration of the ethanol solvent through 0 ml, 0.5 ml, 1.0 ml, 1.5 ml, and 2.0 ml. The as deposited film samples were allowed to cool to room temperature after which they were placed in petri dishes before undergoing film characterisation as follows:

2.1. Structural characterisation of SnS thin film semiconductor

i) X ray diffraction (XRD)

The crystal phase and other structural parameters analysis were carried out at room temperature using an X-ray diffractrometer (D8 Advance, Bruker AXS, 40Kv, 40 mA) with monochromatic CuKα (λ=1.540598 Å) over a scan mode of step size 0.034˚ and counts accumulated for 192.1 s at each step for 2θ ranging from 20˚ to 80˚. The XRD diffractogram was obtained using Origin Pro 2018 software with the FWHM for the peaks estimated using a Gaussian function. Results were analysed with the scientific graphing analysis software and phase identification was done using the inorganic crystal structure data (ICSD) pattern [7] after which the crystallite size, inter atomic spacing (d-spacing), lattice parameter, dislocation density and micro strain were calculated and analysed using appropriate equations /relations.

a) Lattice Parameter

The lattice parameters a, b and c value for the orthorhombic crystallographic system of Tin (II) sulphide thin film was calculated from the observed values of 2θ using d values (interplaner spacing) for the orthorhombic structure [12]:

$$1/d^2_{hkl} = h^2/a^2 + k^2/b^2 + l^2/c^2 \quad (1)$$

Where d is the space between lattice planes and h k l are the miller indices.

b) d-Spacing

The atomic spacing parameter d was estimated from the Bragg's equation [9]:

$$2d \sin\theta = n\lambda \quad (2)$$

$$d = \frac{\lambda}{2\sin\Theta} \quad (3)$$

Where n=1, λ=1.5406A^0

c) Crystallite Size

The average crystallite size of the film was calculated using Debye Scherer's formula [9]: Crystallite size (D) $=\frac{K\lambda}{\beta Cos\theta}$, which can also be written as

$$D = \frac{0.9\lambda}{\beta\cos\theta} \quad (4)$$

Where β = full width at half maximum (FWHM), θ = diffraction angle, k = Shape factor and λ = wavelength of the X-rays (1.5406 Å) and D= crystallite size respectively.

d) Dislocation Density δ

Dislocation density δ was estimated using [10]:

$$\delta = \frac{1}{D^2} \quad (5)$$

Where D is the grain size of the film

e) Micro Strain ε

The micro-strain ε was estimated using the equation [11] (Where β = FWHM):

$$\varepsilon = \frac{\beta}{4\tan\Theta} \tag{6}$$

f) Texture Coefficient

Quantitative information about the preferential crystallite orientation of the SnS thin films were obtained from the texture coefficient (TC) [12-13]:

$$TC = \frac{I/I_o}{(1/N)\,\Sigma_N\left(I/I_o\right)} \tag{7}$$

Where: I is the measured intensity of the intense peak in the XRD spectrum, I_o is the intensity for completely random sample or the standard intensity of the hkl plane taken from the JCPDS 00-039-0354 card and N is the number of reflections considered in the analysis.

2.2. Scanning electron microscopy (SEM)/energy dispersive spectroscopy (EDS)

The morphology and the microstructure of the SnS thin film was characterized using High Resolution Scanning Electron Microscopy (HR-SEM, Zeiss) while the elemental composition of the films were determined by an Energy dispersive X-ray spectroscopy (EDS; Oxford instrument). The instrument was operated at a voltage of 20 kV while the images were captured at 5 kV. Average grain size and grain size distribution histogram was obtained using imagej software.

2.3. Surface profilometry

A Profilometry (VEECO DEKTAK 150) was used to carry out measurement of the thickness of the deposited films.

3. Results and discussion

3.1. Surface profilometry and physical properties

The thickness of the as deposited SnS thin films as obtained from surface profilometry are 0.20 µm, 0.25 µm, 0.30 µm, 0.35 µm and 0.40 µm. The deposited films were smooth and strongly adherent to the surface of the substrate. A colour change was observed with increase in film thickness from 0.20 µm to 0.40 µm. The colour changed from pale yellow to gray via brown with the increase of film thickness. The SnS films grown at lower thickness of 0.20 µm, 0.25 µm, and 0.30 µm were more transparent than the films grown with thickness of 0.35 µm and 0.40 µm. Fig 1, shows the as deposited SnS thin films of 0.20 µm, 0.25 µm, 0.30 µm, 0.35 µm and 0.40 µm thickness.

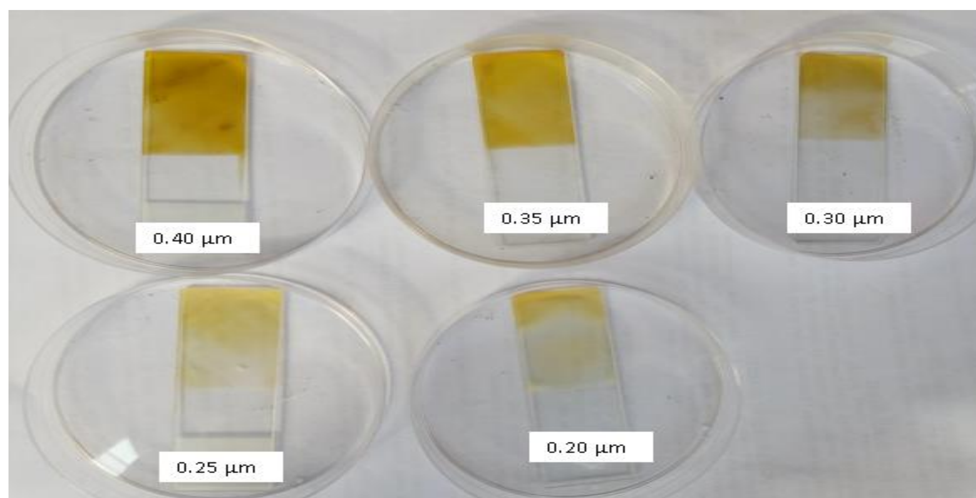

Fig. 1: Shows the As Deposited SnS Thin Films of 0.20 µm, 0.25 µm, 0.30 µm, 0.35 µm and 0.40 µm Thickness.

3.2. Compositional analysis of as deposited SnS thin films (0.2 to 0.4 µm thickness)

Fig 2(a-e) shows the EDX spectrum of the as deposited SnS thin film at thickness of 0.2, 0.25, 0.30, 0.35 and 0.45 µm which reveals that the films are made up of Sn and S elements. Negligible amount of other elements were also observed which could be attributed to the composition of the soda lime glass substrate. These elements include Sodium (Na), Calcium (Ca), Silicon (Si) and Chlorine (CI). The elemental composition of the SnS films in terms of atomic percent (%) is shown in Table 1 while the variation of Sn/S ratio with film thickness is shown in Fig 3.

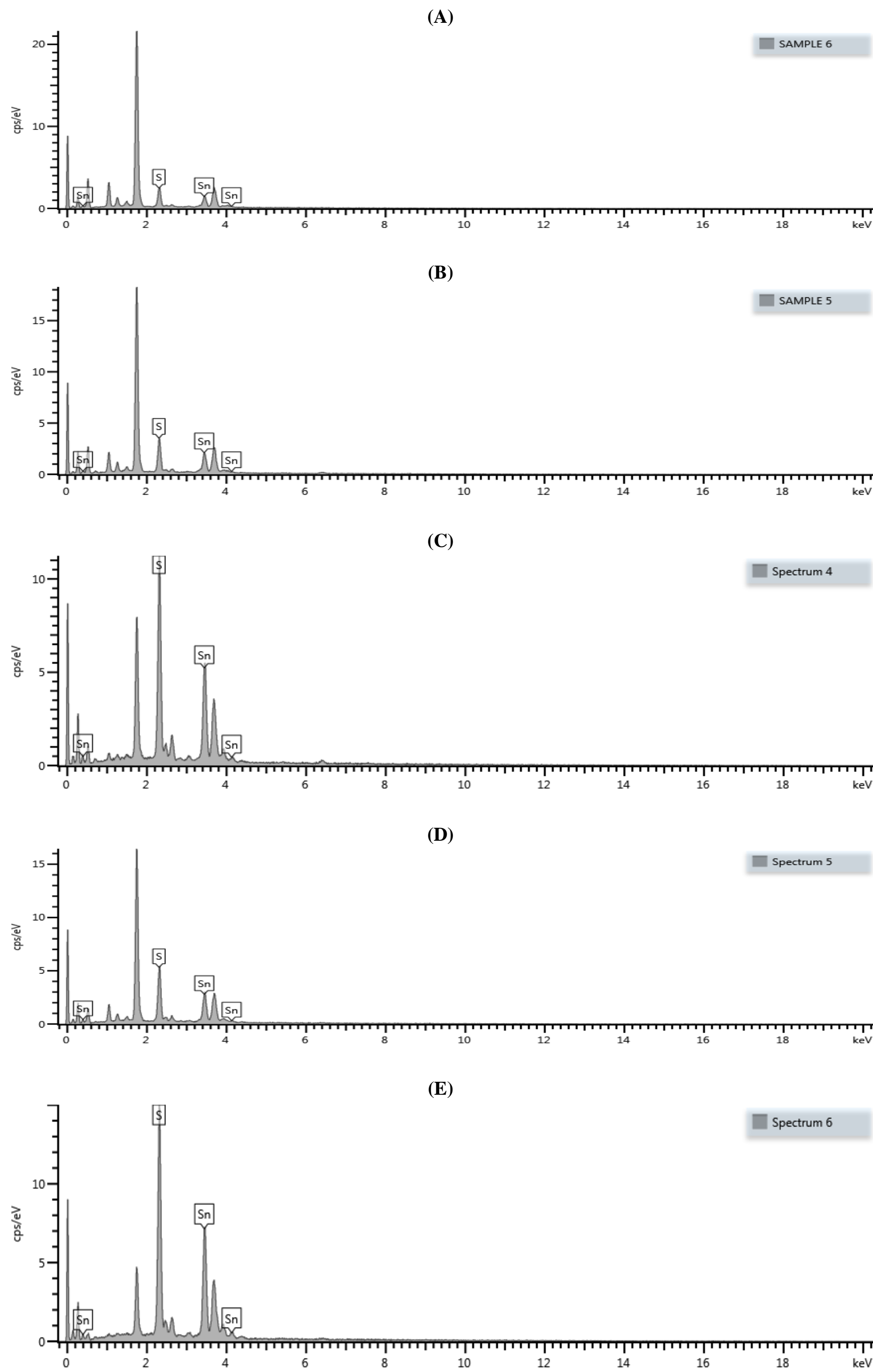

Fig. 2: (A-E): EDS Spectrum of the SnS Thin Films of 0.20 µm, 0.25 µm, 0.30 µm, 0.35 µm and 0.40 µm Thickness.

Table 1: As Deposited SnS Thin Film Composition in Terms of Atomic Percent

Thickness (nm)	Sn (at. %)	S (at. %)	Sn/S at ratio	SnS (Total)
0.20	55.57	44.43	0.80	100
0.25	56.44	43.56	0.77	100
0.30	59.52	40.48	0.68	100
0.35	62.50	37.50	0.60	100
0.40	63.60	36.40	0.57	100

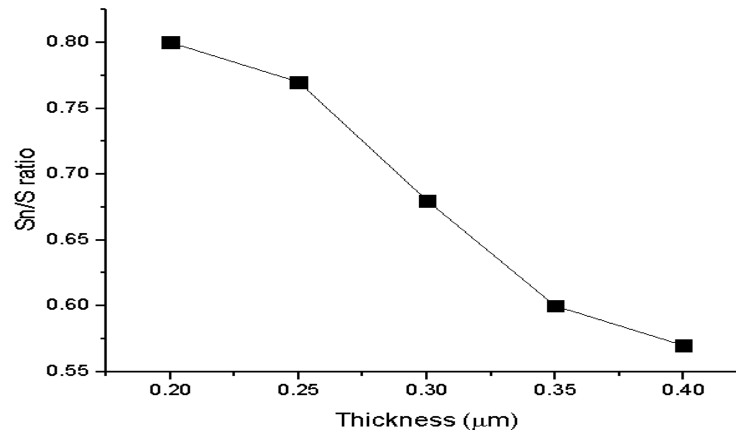

Fig. 3: Sn/S Atomic Percent (at. %) Ratio as a Function of Film Thickness.

From table 1, the sulphur content was observed to increase with increase in film thickness. 0.2 to 0.30 μm film thickness possess lower sulphur content as compared to 0.35 to 0.40 μm higher film thickness. For a film of varying thickness deposited by chemical vapour deposition on a substrate, the substrate temperature is of interest in the formation and determination of the composition of the film as it enhances the kinetics of the film formation. A constant substrate temperature of 258 ℃ was used for the deposition of all the SnS thin film. Sn/S ratio was observed to slightly decrease with increase in SnS film thickness which correlates with the report of [3, 14]. The AACVD deposition method employed involves chemical reactions with precursors, mostly reacting components undergoing reaction at the substrate surface or in the vicinity of the substrate. As a result the evaporated sulphur and tin atoms reaches the substrate surface with different velocities and energies due to their different vapour pressures. Since Sulphur tends to have a greater vapour pressure compared to tin, more of the sulphur atoms will arrive on the substrate than tin as observed in table 1. Some of the S atoms are scattered back on arrival at the substrate surface which could be attributed to adatom mobility, lower sticking coefficient or heat radiant effect between the substrate surface and the deposited SnS thin film hence resulting in lower sulphur content or a large deficiency at lower thickness as compared to higher thickness. The effect however reduces at higher thickness as a result of reduction in scattering loss due to a decrease in heat gradient with the formation of clusters of SnS crystallites at higher thickness and correlates with the findings of [15].

3.3. X-ray diffraction (XRD) analysis

Fig 4 shows the XRD pattern of SnS thin films of 0.20 μm, 0.25 μm, 0.30 μm, 0.35 μm and 0.40 μm thickness.

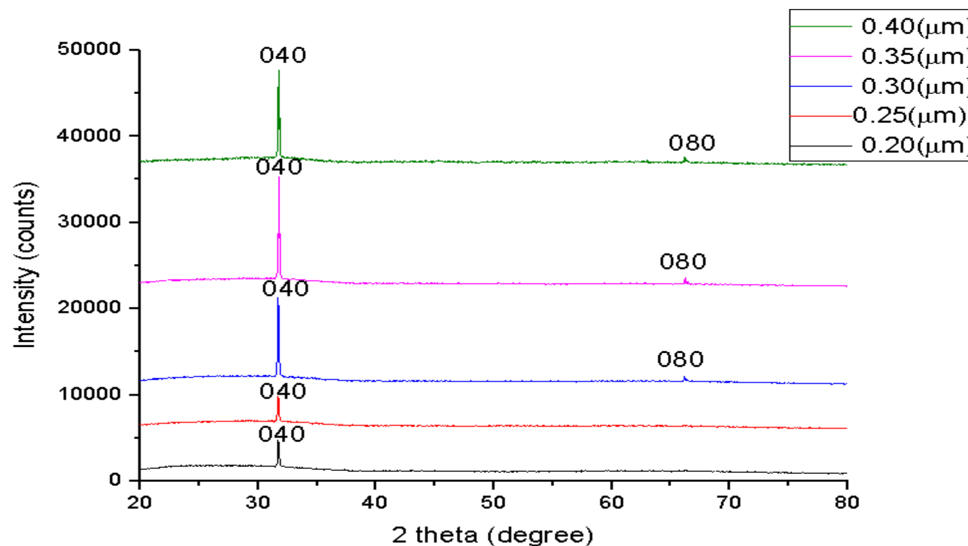

Fig. 4: XRD Pattern for SnS Thin Films of 0.20 μm, 0.25 μm, 0.30 μm, 0.35 μm and 0.40 μm Thickness.

The XRD spectrum scan over the range of $20° \leq 2\Theta \leq 80°$ of the SnS films grown at 0.2, 0.25, 0.30, 0.35 and 0.40 μm is shown in Fig 4. The observed peaks for all the films have been analysed and indexed using standard pattern for the mineral herzenbergite with orthorhombic structured SnS (JCPDS PDF card 39-0354). The analysis of the XRD pattern of the film indicates formation of a poorly crystalline films due to the formation of few peaks. The films grown at lower thickness of 0.2 and 0.25 μm showed only one peak at 2Θ approximately 31.7 ° diffracted along the (040) plane which appears like a single crystal in nature or a single broad poorly defined crystalline peak with other peaks been totally suppressed which could be attributed to short range ordering among the film atoms at the thickness range. The absence of peaks at 0.20 and 0.25 μm thickness suggest a poor crystalline or nearly amorphous nature of the SnS thin film at these thickness which is peculiar to chalcogenides grown at room temperature [14.16]. However, the SnS thin films of 0.30, 0.35 and 0.40 μm thickness exhibited few peaks at 2Θ approximately 31.7 ° and 66.6 ° diffracted along the (040) and (080) plane respectively which could signify that atomic ordering increases with increase in film thickness. The films tend to have a preferred orientation along the (040) plane. There is no variation in peak position with increase in thickness; but there is increase in intensity with increase in film thickness. The broad peak situated at a small diffraction angle is specific to the amorphous or poorly crystalline network, increase in the thin film thickness improves crystallinity and the peaks become more intense and narrower.

3.3.1. D spacing

The observed d spacing as compared to the standard d spacing is shown in table 2

Table 2: Observed and Standard D Spacing for Varied SnS Thin Film Thickness

S/n	Film thickness (μm)	2Θ	Observed D spacing (°A)	Standard D spacing (°A)
1	0.20	31.70270	2.8201	2.8000
2	0.25	31.70273	2.8201	2.8000
3	0.30	31.75743	2.8154	2.8000
4	0.35	31.74203	2.8167	2.8000
5	0.40	31.73912	2.8170	2.8000

A slight difference occurs in the values of the observed d spacing as compared to the standard d spacing which could be attributed to the presence of unit cell volume contraction that might signify the presence of strain in the films

3.3.2. Texture coefficient

The calculated texture coefficient values of the five samples is given in table 3.

Table 3: Calculated Texture Coefficient for the Varied SnS Thin Films Thickness

S/N	Thickness Mm	Texture coefficient (TC)	
		TC (040)	TC(080)
1	0.20	1.00	_
2	0.25	1.00	_
3	0.30	1.16	0.84
4	0.35	1.22	0.78
5	0.40	1.25	0.75

The value obtained shows that all the TC values of (040) plane of SnS thin film component are larger than 1 which indicates that all the SnS films are polycrystalline with preferred orientation along the (040) plane which denotes that the number of grains along this plane is more than that on the other planes [12], [13], [17] and the degree of preferential orientation (DPO) increased with increase in thickness.
The summarised structural parameters of the films is given in table 4 while Fig 5 shows the variation of average crystallite size with thickness. The parameters were calculated along the preferred orientation defined by the texture coefficient

Table 4: Summary of Calculated Structural Parameters for 0.2, 0.25, 0.30, 0.35 and 0.4 μm SnS Thin Film Thickness

S/n	Thickness (μm)	Full width half maximum $\boldsymbol{\beta}$ (°)	2Θ (°)	Grain size D (nm)	Dislocation density $\boldsymbol{\delta} \times \mathbf{10^{14}}$ (Lines/$\mathbf{m^2}$)	Micro strain $\times \mathbf{10^{-4}}$
1	0.40	0.13633	31.73912	60.57	2.73	5.72
2	0.35	0.13935	31.74203	59.26	2.85	5.84
3	0.30	0.14260	31.75743	57.94	2.98	5.99
4	0.25	0.14629	31.70273	56.44	3.14	6.13
5	0.20	0.15030	31.70270	54.94	3.31	6.30

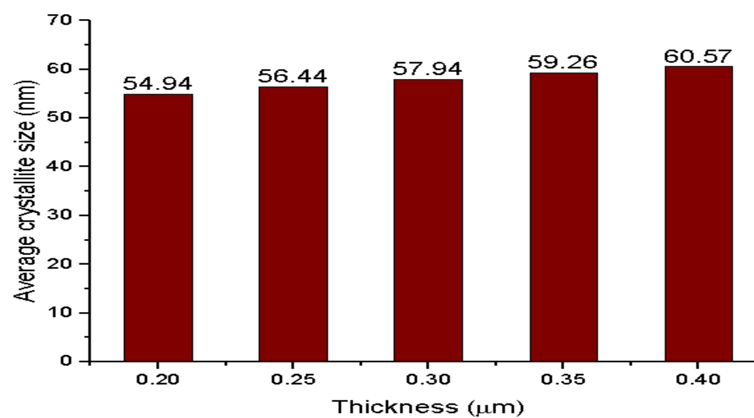

Fig. 5: Composite Variation of Average Crystallite Size with Thickness.

The average crystallite size was calculated using the full width at half maximum of the most preferred orientation (040) which is also the most intense peak by the Scherer formula. The average crystallite size was found to increase with increase in thickness of the films. Increase in thickness enhances the presence of several grown atomic layers thereby creating gain in thermal energy which facilitates their restructuring leading to enlargement of crystal size and the reduction of crystal defects. From table 2, the decrease of full width at half maxima (FWHM) with increase in film thickness reflects the decrease in number of lattice imperfections in the deposited SnS thin film due to significant decrease in the internal micro strain in the film.
The average crystallite size of the films increased from 54.4 nm to 60.57 nm with increase in film thickness from 0.2 to 0.40 μm. The low value of 54.4 nm for the lower thickness of 0.2 μm could be attributed to reduction in growth of deposited atoms due to reduction in the formation of nuclides as a result of inadequacy of material for film formation and bonding between the nuclides and substrate surface which could restricts in-part the mobility of deposited growth atoms. However the formation of nuclide tends to increase with increase in SnS film thickness with a reduction in the interactions between the substrate surface and the deposited film layer, hence leading to the merging of smaller crystallites into larger ones as a result of potential energy difference between small and large particles [14, 18].
Poor crystallinity in the thinner films of 0.2 to 0.25 μm could also be associated with an incomplete growth of the crystallites as only few atomic layers of disordered atoms constitute the bulk of the SnS film at lower thickness while for thicker films there are growth of sever-

al atomic layers which results in gain in thermal energy that could enhance their restructuring for enlargement of crystal size and reduction of crystal defect. Increase in film thickness enhances increase in crystallite size due to formation of larger grains on the surface of smaller grains.
Furthermore, the mechanism of thin film crystal growth assumes that the growing faces of crystallites often corresponds to the crystal shape at equilibrium and are determined by the crystal orientation [19]. As a result a thin film growth competition often arises among neighbouring crystals in line with their respective growth orientation so as to enhance the growth of faster crystals over the slower ones which signifies a selection of film orientation so as to encourage enhanced growth texture thereby increasing the crystallinity of the deposited films with increase in thickness of films from 0.2 µm to thicker films of 0.40 µm. The 0.40 µm thickness has the largest crystallite size and hence could exhibit the most crystallinity.

3.3.3. Dislocation density and micro strain

Fig 6 and Fig 7 shows the composite variation of dislocation density with thickness and the composite variation of micro strain with thickness.

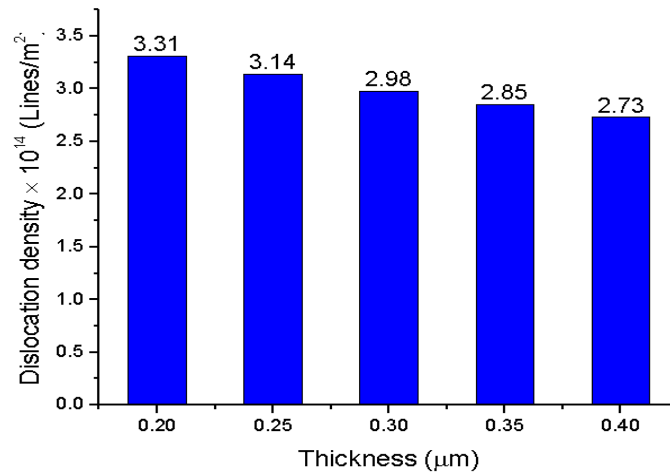

Fig. 6: Composite of Dislocation Density as A Function of Thickness.

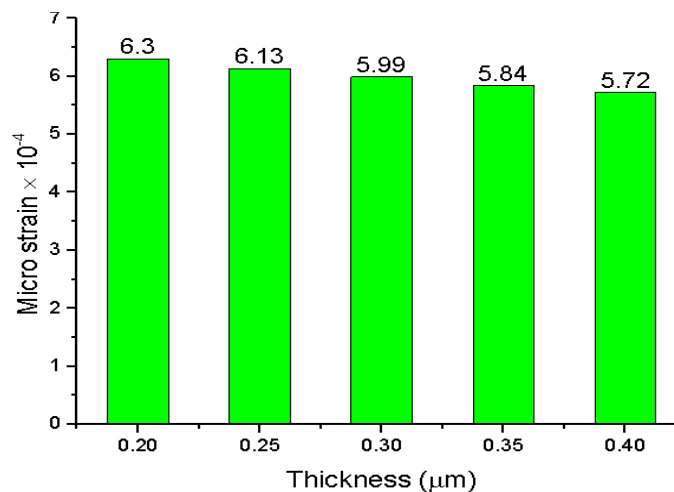

Fig. 7: Composite of Micro Stain as A Function of Thickness.

There is a decrease in micro strain and dislocation density with increase in film thickness from Fig 6 and 7. The decrease could be attributed to the release of stress in the films by simultaneous annealing during deposition of the films leading to improvement in the crystallinity of the films with increase in thickness [20]. The decrease could also be attributed to reduction in the inter-planar spacing which reduces the irregularity in the planar stacking sequence of atoms in the films hence increasing the crystallinity of the deposited films with increase in film thickness.

3.4. Scanning electron microscopy (SEM)

The surface morphology of the as deposited SnS thin films of 0.2, 0.25, 0.30, 0.35 and 0.40 µm thickness as examined with SEM is shown in Fig 8 (a-e). The average grain size of the SnS thin films were calculated using imageJ software [21]. Otsu's thresholding method and particle analysis [22] was used after which statistical analysis of the data was made with histogram generated to study the grain distribution and average grain size determine from the average particle size assuming round/spherical particles as confirmed by the analysis. The particle analyser was configured in a size range of 0 nm^2 to infinity in other to allow for coverage of smaller particles.
The SnS films of 0.2 to 0.40µm thickness exhibited two distinguishable microstructural features consisting of a portion of agglomerates and some defined spherical grains. The agglomerates increases for films of 0.2 to 0.30 µm thickness after which it decreases for films of 0.35 to 0.40 µm thickness leading to a more defined grain structure and growth for the films of 0.40 µm thickness. The SnS films of 0.2 to 0.30 µm thickness exhibited a non-uniformly distributed grain sizes. No visible crack or hole was observed as the films were randomly directed on the surface of the SnS films. As the thickness increases, the deposited SnS thin film tends to have a porous and uneven grain

growth leading to an uneven film surface and poor surface morphology of the deposited films. With increase in SnS film thickness to 0.35 and 0.40 μm, the films contain more uniform and tightly bonded grains with the most improved grain and crystal structure been at the thickness of 0.40 μm.

Furthermore with increase in film thickness, the deeper layers of film atoms are subjected to stronger interatomic forces to form a compact structure, while for a thinner film the atoms near the surface are subjected to weaker interatomic forces to form a loosely packed structure.

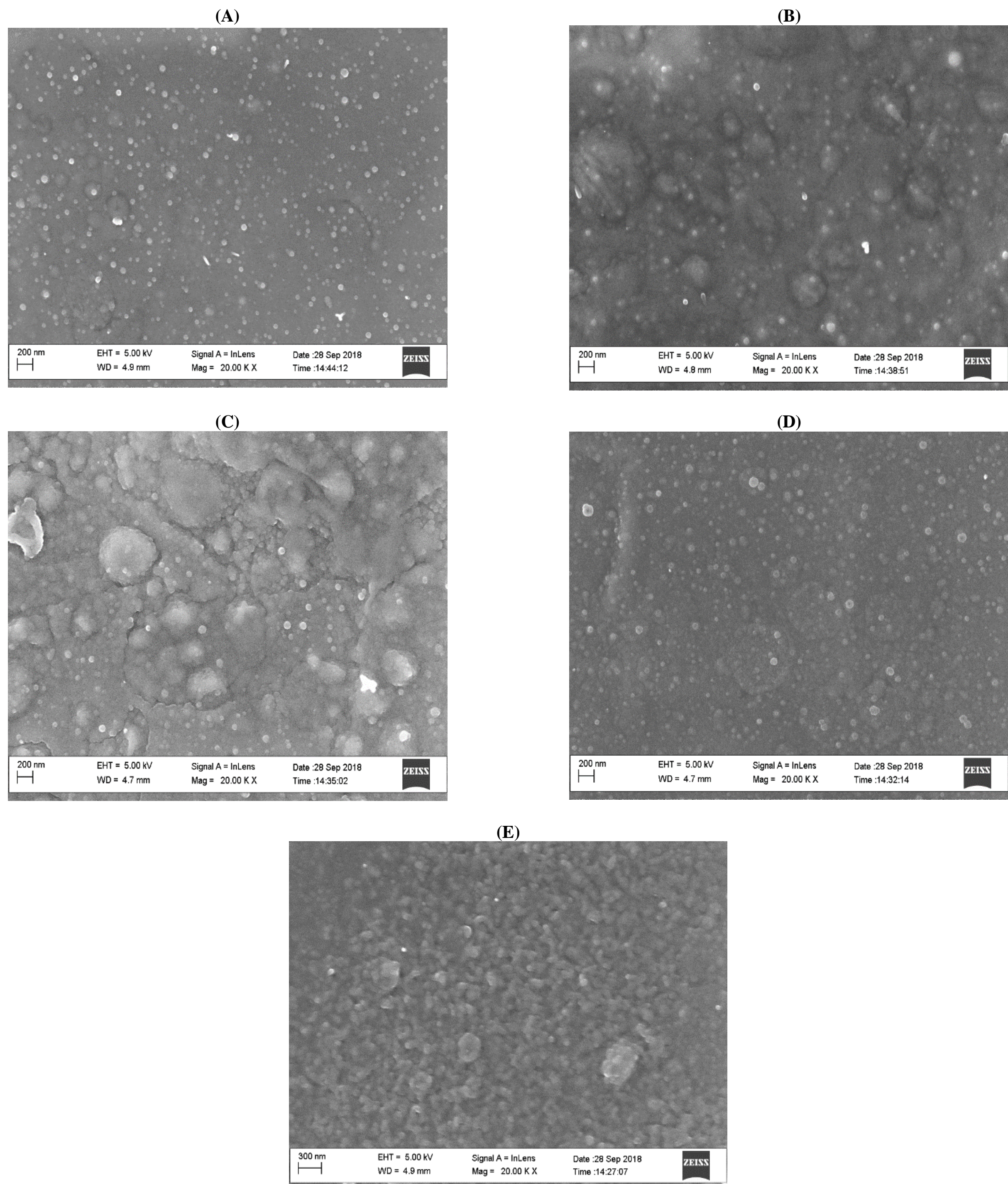

Fig. 8: (A-E). The Surface Morphology of the as Deposited SnS Thin Films of 0.2, 0.25, 0.30, 0.35 and 0.40 μm Thickness.

The grain size distribution histogram plot for SnS samples of 0.2, 0.25, 0.30, 0.35 and 0.40 μm thickness is shown in Fig 9 while the composite average grain size plot for 0.2, 0.25, 0.30, 0.35 and 0.40 μm thickness is shown in Fig 10.

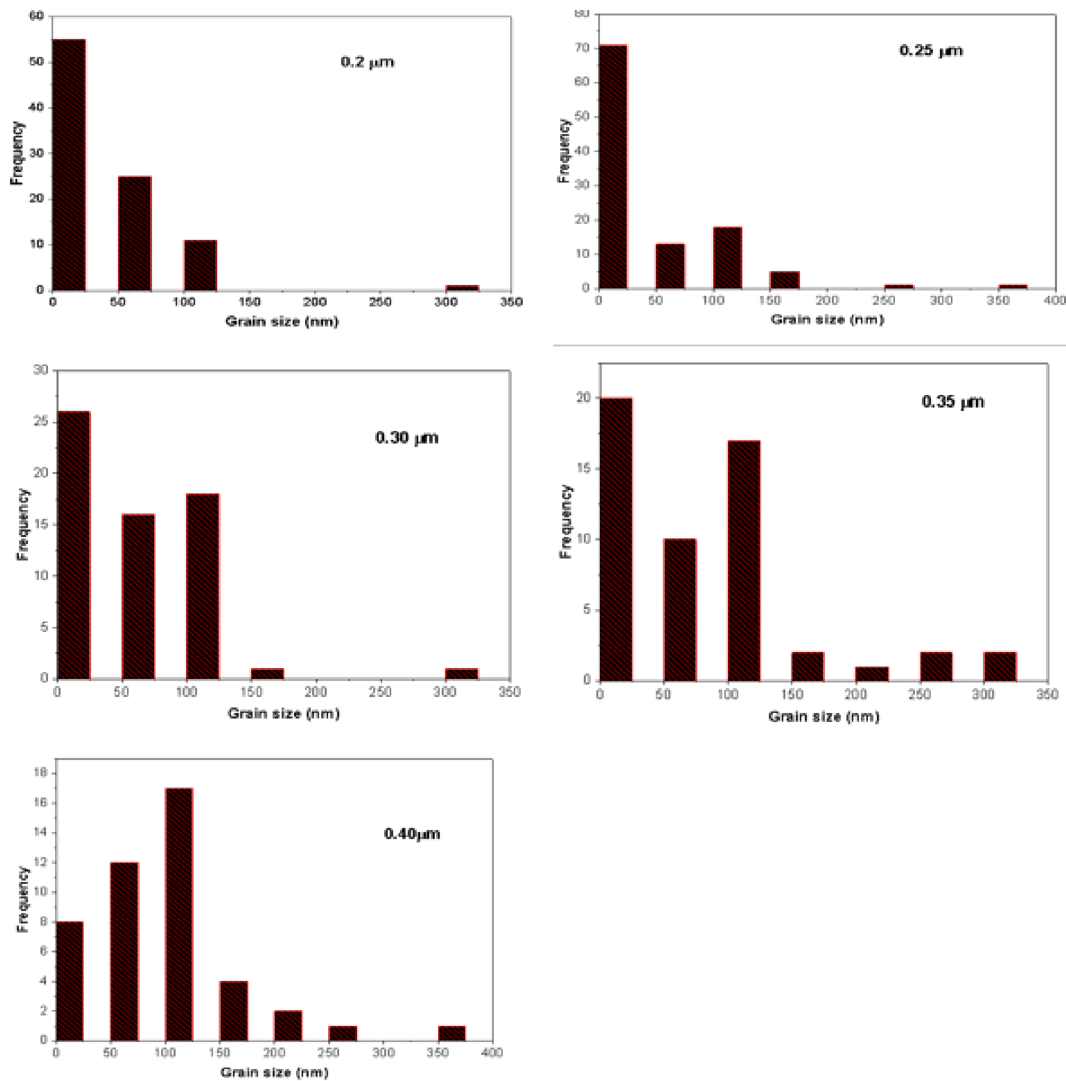

Fig. 9: Grain Size Histogram Plot for Sns Samples of 0.20, 0.25, 0.30, 0.35 and 0.40µm.

From Fig 9, the histogram shows a non-uniform grain concentration and distribution at grain size range of 0.0 to 100 nm for all the as-deposited SnS thin films. The grain size distribution at 0.0 to 100 nm is larger than that of 100 to 400 nm range. A preferred grain distribution and growth defining factor or pattern exist at 100 nm for all the films which could be related to the preferred crystal growth orientation earlier defined by the XRD results. The preferred grain distribution increases with increase in film thickness, with the most prominent distribution at the film of 0.4 µm thickness. The increase in grain distribution from 0 to 100 nm range is followed by a decrease from 100 to 400 nm for the 0.4 µm thickness which could be attributed to initialisation of grain stability and uniformity at the range of 250 to 400 nm. The absence of grain at 300 nm within the range of 250 to 400 nm of the 0.4 µm thickness could be attributed to grain boundary effect or the presence of crystal defect. The as-deposited 0.4 µm thickness shows a more uniform grain distribution and growth which could signify an optimum for the as deposited SnS films as the larger grains could reduce the number of grain boundaries and charge trap density hence allowing charge carriers to move freely in the lattice thereby causing a reduction in resistivity and increase in conductivity of the films.

Fig 10 shows that the average grain size which is as labelled on each column increases with increase in film thickness.

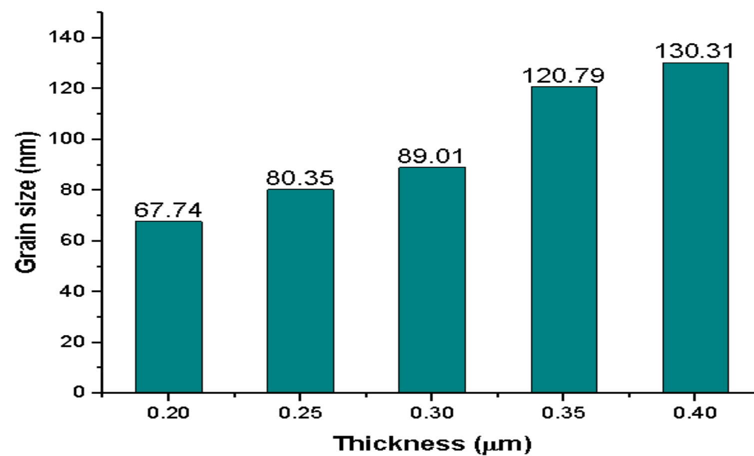

Fig. 10: Composite Average Grain Size Plot for 0.20, 0.25, 0.30, 0.35 and 0.40µm SnS Thin Film Thickness.

As judged from the XRD results, increase in thickness of SnS films from 0.30 to 0.40 µm leads to formation of polycrystalline films. The polycrystalline thin films consist of crystallites joined together by the grain boundaries [23]. The grain boundary regions are disordered regions, characterized by the presence of a large number of defect states due to incomplete atomic bonding or departure from stoichiometry for compound semiconductors which serve as carrier traps with a density dependent on the film thickness. Increase in SnS film thickness could necessitate the growth of smaller grains into larger grains which due to the coalescence of small grains into bigger grains with an evident improvement in the film grain size which are more densely packed leading to the reduction in grain boundaries and potential barrier thereby produces changes in the structure and phase of the films which will in essence affects electrical conductivity and the energy band gap of the SnS thin film which are important parameters in the usage of SnS as a semiconductor channel layer hence buttressing the choice of 0.4 µm thickness as optimum for use as a semiconductor channel layer in a transistor. The larger grain sizes could enhance reduction in grain boundaries and potential barrier there by releasing charge carriers that were trap so as to further enhance carrier conductivity.

4. Conclusion

The SnS thin film semiconductors of 0.20, 0.25, 0.30, 0.35 and 0.40µm SnS thickness were deposited using Aerosol assisted chemical vapour deposition (AACV). The SnS thin films were found to be poorly crystalline consisting of Sn and S elements in varying composition with increase in thickness. No noticeable change was noticed in the crystal structure of the films. No impurities peaks of elemental sulphur, tin or other tin sulphide phases were identified in the XRD pattern of the films which signifies the formation of pure SnS phase. The preferred orientation of all the films was found to be along the (040) plane. Increase in the thickness of the films from 0.20 through 0.40 µm enhances the crystallinity of the SnS thin film samples by increasing the number of crystallites which is also buttress by the decrease of dislocation density and micro strain for SnS thin film samples of 0.20 to 0.40 µm thickness. A gradual change was observed from the SEM micrographs in the growth of grains of SnS films. Increase in thickness enhances increase in grain size leading to the reduction in grain boundaries and potential barrier which in essence will affects the electrical conductivity and band gap of the SnS thin films and its usage as a semiconductor in a field effect transistor. The film of 0.40 µm thickness showed an optimum structural and microstructural film property for all the analysis hence suitable for use as a semiconductor channel layer in field effect transistor.

Acknowledgements

This research did not receive any specific grant from funding agencies in the public, commercial, or not-for-profit sectors. However authors acknowledged the Staff and management of Alex Ekwueme Federal University Ndufu Alike Ikwo-Ebonyi state, Federal University of Technology Minna, Sheda Science and Technology (SHESTCO) and Namiroch research laboratory Abuja all in Nigeria for availing their laboratories for the films deposition and surface profilometry. The authors also acknowledged iThemba Laboratory South Afica for XRD analysis and the electron microscopy unit of the University of Western Cape, South for the SEM/EDS analysis.

References

[1] H. Du, Xi. Lin, Z. Xu, D. Chu, Electric double layer transistors: a review of recent progress, Journal of Material Science, 1-33. 50(2015) 5641-5673. https://doi.org/10.1007/s10853-015-9121-y.

[2] H. Yuan, H. Liu, H. Shimotani, Liquid gated ambipolar transport in ultrathin films of a topological insulator Bi_2Te_3. Nano letters, 11 (2011), 2601-2605. https://doi.org/10.1021/nl201561u.

[3] T.S. Reddy, M.C. Kumar, Co-evaporated SnS thin films for visible light photodetector applications, Royal Society Advances. 6(2016), 95680-95692. https://doi.org/10.1039/C6RA20129F.

[4] P. Thiruramanathan, G.S. Hikku, R. Krishna-Sharman, M. Siva Shakthi, Preparation and characterisation of indium doped SnS thin films for solar cell applications, Journal of Chemical Technology Research, 1(2015),59-65.

[5] S.S. Hedge, A.G. Kunjomana, K.A. Chandrasekharam, K. Ramesh, M. Prashantha, Optical and electrical properties of SnS semiconductor crystals grown by physical vapour deposition technique, Physica B, 406, (2011), 1143-1148. https://doi.org/10.1016/j.physb.2010.12.068.

[6] M. Miyasaka, T. Komatsu, W. Itoh, A. Yamaguchi, H. Ohshima, Effects of semiconductor thickness on poly-crysttalline silicon thin film transistor, Japanese journal of Applied Physics, 35(1), 1-2. https://doi.org/10.1143/JJAP.35.923.

[7] A. Sugaki, A. Kitakaze, H. Kitazawa, Sugaki, A., Kitakaze, A., & Kitazawa, H, Synthesized tin and tin-sulfide minerals; Synthetic sulfide minerals (XIII), Science Reports of the Tohoku University 16(3), 1985, 199–211.

[8] T.H. Patel, Influence of deposition time on the structural and optical properties of chemically deposited SnS thin films, the open surface science journal, 4 (2012), 6-13. https://doi.org/10.2174/1876531901204010006.

[9] B.J. Babu, A. Maldonado, S. Velumani, R. Asomoza, Electrical and Optical properties of Ultrasonically Sprayed Al-doped Zinc Oxide Thin Films, Material Science & Engineering B,10 (2010), 25-30.

[10] I. Ilican, Y. Caglar, M. Caglar, Preparation and Characterization of ZnO Thin Films Deposited by Sol-gel spin coating method, Journal of Optoelectronics and Advanced Materials, 10(10), 2578-2583.

[11] S.M. Ahmed, L.A. Latif, A.K. Salim, The effect of substrate temperature on the optical and structural properties of Tin sulphide thin films, Journal of Basrah research (sciences), 37(2011),1-6.

[12] E. Guneri, F.Gode, C. Ulutas, F. Kirmizigul, G. Altindemir, C. Gumus, Properties of P-type SnS thin films prepared by chemical bath deposition, Chalcogenide letters, 7(2010),685-694.

[13] J. Lv, Z. Zhou, F. Wang, C. Liu, W. Gong, J. Dai, X. Chen, G. He, S. Shi, X. Song, Z. Sun, F. Liu, Effect of annealing temperature and CuO on microstructure and optical band gap of $Cu_xZn_{1-x}O$ thin films, Super lattices and microstructures, 61(2013), 115-123. https://doi.org/10.1016/j.spmi.2013.06.010.

[14] M. Devika, N.R. Koteeswara, K. Ramesh, K.R. Gunasekhar, E.S.R. Gopal, R.K.T. Ramakrishna, R.K.T, Influence of annealing on the physical properties of evaporated SnS films, Semiconductor science and technology, 21(2006), 1125-1131. https://doi.org/10.1088/0268-1242/21/8/025.

[15] A. Gomez, H. Martinez, M. Calixto-Rodriguez, D. Avellaneda, P.G. Reyes, O. Flores, A study of the structural, optical and electrical properties of SnS thin films modified by Plasma, Journal of materials science and engineering, 33 (6), 2013, 352-358.

[16] P. Jain, P.Arun, Parameters influencing the optical properties of SnS thin films. Journal of semiconductors, 34 (2013), 1-6. https://doi.org/10.1088/1674-4926/34/9/093004.

[17] M. Safonova, P.P.K. Nair, E. Mellikov, R.Aragon, K. Kerm, R. Naidu, O. Volobujeva, Thermal annealing of sequentially deposited SnS thin films. Proceedings of the Estonian academy of sciences, 64(4), 2015, 488-494. https://doi.org/10.3176/proc.2015.4.04.

[18] G.D. Deshmukh, S.M. Patil, S.S. Patil, P.H. Pawar, Effect of film thickness on structural and optical properties of Bi_2Te_3 thin films, Journal of chemical, biological and physical sciences: section c, 5(3), 2015, 2769-2779.

[19] H. Jian, S. Cheng, X. Wu, Y. Yang, Effect of annealing temperature on electrical and optical properties of SnS:Ag thin films, Natural science, 2(2010), 197-200. https://doi.org/10.4236/ns.2010.23030.
[20] Y. Chen, I. Shih, Scaling down of organic thin film transistors: Short channel effects and channel length dependent field effect mobility, Journal of material science, 44 (2009) 280-284. https://doi.org/10.1007/s10853-008-3047-6.
[21] W.S. Rasband, ImageJ, National institute of health, Bethesda, Maryland, USA, http://imagej.nih.gov/ij/1997-2014.
[22] G. Julio, M.D. Merindano, M. Canals, M. Rallo, Image processing techniques to quantify micro projections on outer corneal epithelial cells, Journal of Anatomy, 212(2008), 879-886. https://doi.org/10.1111/j.1469-7580.2008.00898.x.
[23] S.J. Ikhmayies, R.N. Ahmad-Bitar, The Influence of Substrate Temperature on the Photovoltaic properties of Spray-deposited CdS: In Thin Films, Applied Surface Science, 256 (2010), 3541-3545. https://doi.org/10.1016/j.apsusc.2009.12.104.